NIH Public Access
Author Manuscript
Plant J. Author manuscript; available in PMC 2013 April 29.

Published in final edited form as:
Plant J. 2009 July ; 59(2): 344–358. doi:10.1111/j.1365-313X.2009.03862.x.

Tandem affinity purification and mass spectrometric analysis of ubiquitylated proteins in Arabidopsis

Scott A. Saracco[1,†], **Maria Hansson**[1], **Mark Scalf**[2], **Joseph M. Walker**[1], **Lloyd M. Smith**[2], and **Richard D. Vierstra**[1,*]

[1]Department of Genetics, University of Wisconsin-Madison, Madison, WI 53706-1574, USA

[2]Department of Chemistry, University of Wisconsin-Madison, Madison, WI 53706-1574, USA

SUMMARY

Protein ubiquitylation is a central regulatory mechanism that controls numerous processes in plants, including hormone signaling, developmental progression, responses to biotic and abiotic challenges, protein trafficking and chromatin structure. Despite data implicating thousands of plant proteins as targets, so far only a few have been conclusively shown to be ubiquitylated *in planta*. Here we describe a method to isolate ubiquitin–protein conjugates from Arabidopsis that exploits a stable transgenic line expressing a synthetic poly-*UBQ* gene encoding ubiquitin (Ub) monomers N-terminally tagged with hexahistidine. Following sequential enrichment by Ub-affinity and nickel chelate-affinity chromatography, the ubiquitylated proteins were trypsinized, separated by two-dimensional liquid chromatography, and analyzed by mass spectrometry. Our list of 54 non-redundant targets, expressed by as many as 90 possible isoforms, included those predicted by genetic studies to be ubiquitylated in plants (EIN3 and JAZ6) or shown to be ubiquitylated in other eukaryotes (ribosomal subunits, elongation factor 1α, histone H1, HSP70 and CDC48), as well as candidates whose control by the Ub/26S proteasome system is not yet appreciated. Ub attachment site(s) were resolved for a subset of these proteins, but surprisingly little sequence consensus was detected, implying that specific residues surrounding the modified lysine are not important determinants for ubiquitylation. We also identified six of the seven available lysine residues on Ub itself as Ub attachment sites, together with evidence for a branched mixed-linkage chain, suggesting that the topologies of Ub chains can be highly complex in plants. Taken together, our method provides a widely applicable strategy to define ubiquitylation in any tissue of intact plants exposed to a wide range of conditions.

Keywords

ubiquitin; post-translation modification; mass spectrometry; Arabidopsis

INTRODUCTION

Plants, like other eukaryotes, exploit a wide variety of post-translational modifications to regulate the activity, location and/or half-life of their constituent proteins. One of the most

© 2009 The Authors

*For correspondence (fax +1 608 262 2976; vierstra@wisc.edu).
†Present address: Monsanto Company, Chesterfield, MO 63017, USA.

SUPPORTING INFORMATION

Additional Supporting Information may be found in the online version of this article:

Please note: Wiley-Blackwell are not responsible for the content or functionality of any supporting materials supplied by the authors. Any queries (other than missing material) should be directed to the corresponding author for the article.

NIH-PA Author Manuscript
NIH-PA Author Manuscript
NIH-PA Author Manuscript

NIH-PA Author Manuscript

NIH-PA Author Manuscript

NIH-PA Author Manuscript

prevalent modifications involves the covalent attachment of the 76-amino-acid protein ubiquitin (Ub) to accessible lysines in other intracellular proteins (Smalle and Vierstra, 2004; Dreher and Callis, 2007). This ubiquitylation can alter the target in a number of ways depending on the target and the architecture of the bound Ub, which can be attached either singly or as polymeric chains that are internally linked through lysines within Ub itself. The best understood consequence of ubiquitylation is to direct short-lived proteins to the 26S proteasome for subsequent breakdown. Here, poly-Ub chains linked via Lys48 are selectively conjugated to proteins destined for turnover; these poly-ubiquitylated proteins are recognized and degraded by the 26S proteasome, with the concomitant release of the Ub moieties for re-use. It has been estimated that most short-lived cytoplasmic and nuclear proteins are removed by this mechanism (Vierstra, 2003). Other roles for Ub addition include modifications of chromatin structure and vesicular trafficking by mono-ubiquitylation, and DNA repair and the turnover of plasma membrane-bound receptors and transporters via endocytosis to the lysosome/vacuole after addition of Lys63-linked Ub polymers (Mukhopadhyay and Riezman, 2007).

Accumulating genetic studies have implicated ubiquitylation in the control of almost every aspect of plant biology, including signaling by most (if not all) hormones, light perception, entrainment of circadian rhythms, embryogenesis, responses to adverse environments, protection against pathogens, and epigenetic regulation (Smalle and Vierstra, 2004; Dreher and Callis, 2007). The fact that almost 1700 *Arabidopsis thaliana* genes (>5% of the proteome) have been connected to the production and metabolism of Ub–protein conjugates implies that ubiquitylation rivals phosphorylation in both depth and breadth as the dominant modification in plants (Vierstra, 2009). Even though thousands of intracellular proteins are predicted to be targets, only a handful [e.g. phytochrome A (phyA), auxin/indole-3-acetic acid (AUX/IAA), Della and jasmonic acid/ZIM-containing (JAZ) proteins, long hypocotyl-5 (HY5), abscisic acid-insensitive-5 (ABI5) and histone H2B] have been confirmed via genetic or biochemical methods as ubiquitylated *in vivo* (Vierstra, 2009 and references therein).

Full appreciation of ubiquitylation will ultimately require definition of the plant ubiquitylome, the collection of proteins modified by Ub. Unfortunately, generating this ubiquitylome is complicated by the sheer number of targets whose ubiquitylated forms are typically present at low steady-state levels, and the possibility that individual targets carry varying numbers of Ubs bound by various linkages. One powerful strategy to overcome these challenges is the application of mass spectrometry (MS) to analyze complex protein fractions that are enriched in Ub–protein conjugates. Peng *et al.* (2003) pioneered this approach with the MS analysis of ubiquitylated proteins isolated from a yeast (*Saccharomyces cerevisiae*) strain in which all four native *UBQ* genes were replaced by a single gene expressing 6xHis-tagged Ub. Using as a signature the unique isopeptide-linked Gly-Gly-Lys footprint derived from ubiquitylated proteins after trypsinization, they also determined the Ub attachment site(s) for a subset of these proteins. This and subsequent studies on yeast and mammalian cells (e.g. Hitchcock *et al.*, 2003; Kirkpatrick *et al.*, 2005; Matsumoto *et al.*, 2005; Mayor *et al.*, 2005; Tagwerker *et al.*, 2006) found surprisingly little consensus in the Ub attachment sites, indicating that specific sequences surrounding the accessible lysine are not important determinants for ubiquitylation, except that the lysine must be solvent-exposed. These MS analyses also revealed that polymeric Ub chains can be assembled *in vivo* using any of the seven Ub lysines for concatenation (e.g. Peng *et al.*, 2003), and that highly complex mixed-linkage Ub polymers are possible for substrates ubiquitylated *in vitro* (Kirkpatrick *et al.*, 2006).

Similar MS approaches have recently been adapted to plants. Studies by Maor *et al.* (2007) using Ub-binding domains [the Ub-associated (UBA) domain from the Arabidopsis

NIH-PA Author Manuscript

NIH-PA Author Manuscript

NIH-PA Author Manuscript

deubiquitylating isopeptidase UBP14 (Doelling *et al.*, 2001) or the Ub-interacting motif (UIM) from Arabidopsis RPN10 (Smalle *et al.*, 2003)] for a single affinity enrichment step identified 294 proteins in Arabidopsis suspension cells that may be ubiquitylated, with Ub footprints tentatively located in 56. They also detected Ub linkages to itself for five of the seven available lysines (the exceptions being Lys6 and Lys27), thus confirming that plants, like yeast and animals, exploit several types of Ub polymers. More recently, Manzano *et al.* (2008) used the UBA domain from mammalian p62 to enrich for ubiquitylated species from Arabidopsis seedlings to identify additional candidates by MS. In this case, no Ub footprints were reported. Unfortunately, both lists are missing a number of proteins that are known to be ubiquitylated *in planta*, suggesting that many more targets remain to be identified. Moreover, as the former study used cell suspension cultures (Maor *et al.*, 2007), while the latter used seedlings treated with the 26S proteasome inhibitor MG132 (Manzano *et al.*, 2008), it remains unclear whether some of these conjugates represent ubiquitylated proteins generated as a consequence of the stress induced by the cell culture conditions or the inhibitor treatment. In addition, because both studies used a single step for ubiquitylome purification, it is possible that some candidates represent contaminating species that non-specifically bind to the Ub-affinity matrices.

Here we describe a tandem purification method first developed for yeast (Mayor and Deshaies, 2005; Mayor *et al.*, 2005) to enrich more highly for Ub conjugates from intact plants in the absence of 26S proteasome inhibitors. It involved the creation of phenotypically normal Arabidopsis lines that stably express a Ub variant with a 6xHis tag designed to extend from Ub polymers. Ubiquitylated proteins were then enriched from intact untreated plants using a combination of Ub-affinity and nickel-chelate affinity chromatography, with the latter performed under strong denaturing conditions. Initial analysis of these preparations by multi-dimensional protein identification technology (MudPIT) MS identified a list of 54 non-redundant ubiquitylated proteins, with Ub footprint(s) for 13. Importantly, this collection includes a number of proteins that have been predicted to be ubiquitylation targets by genetic analyses or by comparison with the yeast/mammal ubiquitylomes, or that are known to be short-lived. We also identified Ub footprints for all Ub lysines except Lys27, and obtained evidence for a branched mixed-linkage Ub chain, suggesting that highly complex chain topologies are possible. Using this strategy, it should now be possible to more accurately define the ubiquitylome from any plant tissue exposed to a wide range of growth conditions or treatments.

RESULTS

Transgenic plants expressing 6xHis-tagged Ub

To better catalog the plant ubiquitylome, we developed a general-use strategy for improved purification of Ub conjugates that could be readily adapted to any tissue or growth conditions without the potential artifacts inherent in using 26S proteasome inhibitors. Whereas previous attempts employed the Ub-binding domains UBA or UIM (Harper and Schulman, 2006) for a single enrichment step (Maor *et al.*, 2007; Manzano *et al.*, 2008), we found that neither approach yielded sufficiently pure preparations when applied to intact non-treated Arabidopsis seedlings. Consequently, we combined this Ub-affinity strategy with that developed by Ling *et al.* (2000), who exploited transgenic plants expressing 6xHis-tagged Ub in combination with immobilized-metal affinity chromatography. When applied to yeast, this sequential chromatography was shown to substantially enrich for Ub conjugates from whole-cell lysates (Mayor and Deshaies, 2005; Mayor *et al.*, 2005).

Ling *et al.* (2000) added the 6xHis tag (MHHHHHH) directly to the N-terminus of Ub, and then expressed this modified Ub in Arabidopsis as an N-terminal extension of luciferase. To improve exposure of the 6xHis tag within poly-Ub chains, they also used a Ub variant in

NIH-PA Author Manuscript

NIH-PA Author Manuscript

NIH-PA Author Manuscript

which Lys48 had been replaced by arginine, which terminates Lys48-dependent poly-ubiquitylation, and thus positions the 6xHis tag at the end of Lys48-linked chains for maximal exposure. Because high-level expression of K48R Ub is detrimental to plant growth, presumably because it prematurely truncates Ub polymerization via Lys48 (Bachmair *et al.*, 1990; Becker *et al.*, 1993; Schlogelhofer *et al.*, 2006), such a strategy was avoided here. Instead, we developed a *UBQ* transgene that expresses wild-type plant Ub with a 13-amino-acid N-terminal extension of six histidines followed by a flexible glycine-rich linker (MHHHHHHGGGGGSA) (Figure 1a), which would hopefully extend beyond the Ub moieties regardless of its position within the Ub polymer or attachment site to the target protein. To provide high-level expression, we then fused six of these coding regions head-to-tail to form a single in-frame poly-*UBQ* transgene that mimics those found naturally in plants (Callis *et al.*, 1995) (Figure 1a).

When the poly-*6His-UBQ* transgene was introduced into Arabidopsis, a number of lines were identified that expressed high levels of 6xHis-tagged Ub protein as determined by the presence of a new anti-Ub and anti-5His immunoreactive species at approximately 7 kDa as compared to free Ub (5.5 kDa) (Figure 1b and data not shown). Accumulation of this species indicated that the initial hexa-Ub translation product was readily processed into Ub monomers by de-ubiquitylating enzymes, and that the 6xHis tag was relatively resistant to proteolytic cleavage (Figure 1b). For some lines, the level of free 6xHis-tagged Ub equaled that of wild-type Ub. Higher-molecular-mass species were also detected in the *6His-UBQ* lines using anti-Ub antibodies (Figure 1b) or the less sensitive anti-5His antibodies (Figure 2a), indicating that this tagged Ub monomer could be incorporated into poly-Ub chains and Ub–protein conjugates *in vivo* (van Nocker and Vierstra, 1993). The species that were most obvious were located at 13–15 kDa; the lower band probably represented the Ub homodimer, the next highest the 6xHis-tagged Ub/Ub heterodimer, and the third more faint species being the 6xHis-tagged Ub homodimer (Figure 1b).

Over-expression of *UBQ* genes can sometimes adversely affect plant development, presumably by co-suppressing the endogenous suite of *UBQ* genes (Becker *et al.*, 1993; R.D.V., unpublished results). Additional adverse phenotypes can be generated by expressing Ub–protein variants, probably as a result of their interference with various aspects of Ub conjugation and metabolism (e.g. Bachmair *et al.*, 1990; Becker *et al.*, 1993; Schlogelhofer *et al.*, 2006; Yin *et al.*, 2007). It is important that the lines expressing high levels of 6xHis-tagged Ub were phenotypically normal under several conditions that are sensitive to perturbations in the plant Ub/26S proteasome system (UPS). For example, the *6His-UBQ* and wild-type Col-0 plants were morphologically indistinguishable throughout their entire life cycle (data not shown). Flowering time under either long or short days, which is highly sensitive to perturbations in the UPS (Jang *et al.*, 2008; Book *et al.*, 2009), was also unaffected by *6His-UBQ* expression. Root growth in the presence of the proteasome inhibitor MG132 (Yang *et al.*, 2004) or the amino acids analogs canavinine (arginine) and *p*-fluorophenylalanine (phenylalanine), which generate abnormal proteins that require the UPS for removal (Yan *et al.*, 2000), was identical (Figure 1c). Similarly, trichrome branching, which is controlled by the UPS via the Ub ligase UPL3 (or Kaktus; Downes *et al.*, 2003), was not significantly affected (Figure 1d).

When two known targets of the UPS [phyA (Clough *et al.*, 1999) and ABI5 (Smalle *et al.*, 2003; Stone *et al.*, 2006)] were analyzed, their stabilities *in planta* were also unchanged by *6His-UBQ* expression. As shown in Figure 1e, the turnover rate of phyA during red-light irradiation of etiolated seedlings and the stabilization of ABI5 in young green seedlings exposed to ABA were indistinguishable in the wild-type and *6His-UBQ* backgrounds.

NIH-PA Author Manuscript

NIH-PA Author Manuscript

NIH-PA Author Manuscript

Enrichment of Ub–protein conjugates

To enrich for ubiquitylated proteins from the *6His-UBQ* plants, we adapted the tandem affinity method that combined Ub-affinity chromatography with nickel/nitrilotriacetic acid agarose (Ni–NTA) chromatography (Mayor and Deshaies, 2005; Mayor *et al.*, 2005). For the studies described here, the source tissue was 10-day-old green Arabidopsis seedlings grown in liquid culture under continuous light. The Ub-affinity step employed a 23 kDa fragment encompassing the two UBA domains from human HHR23A (Raasi *et al.*, 2004), which was expressed recombinantly as a 49.2 kDa fusion to the C-terminus of glutathione *S*-transferase (GST) (hereafter called GST–UBA). In agreement with the results obtained by Maor *et al.* (2007), this GST–UBA column substantially enriched for ubiquitylated species present in both wild-type and *6His-UBQ* seedlings using an aqueous non-denaturing buffer to prepare the crude extracts, followed by a high salt wash (2 M NaCl) and 8 M urea elution. The eluants from both tissue sources were enriched for Ub conjugates as detected immunologically using anti-Ub antibodies following SDS–PAGE, and they were mostly free of other proteins (with the exception of the GST–UBA ligand and its breakdown products) as detected by silver staining of the gels for total protein (Figure 2a). In agreement with the preference of the HHR23A UBA domains for ubiquitylated species carrying Lys48-linked poly-Ub chains, especially those containing four or more Ub monomers (Raasi and Pickart, 2003; Raasi *et al.*, 2004; Mayor *et al.*, 2005), the eluants were enriched for higher-molecular-mass Ub conjugates compared to the free Ub monomer and dimer (Figure 2a). This smear was recognized by anti-5His antibodies (albeit weakly), confirming that these conjugates also contained the 6xHis-tagged Ub variant (Figure 2a).

That the GST–UBA column bound ubiquitylated proteins in addition to free poly-Ub chains was confirmed by enrichment of phyA–Ub conjugates (Clough *et al.*, 1999). Formation of these conjugates was first induced in etiolated seedlings by a 1 h red-light irradiation, and then these conjugates were enriched from crude extracts using the GST–UBA column and detected following SDS–PAGE by immunoblot analysis with an anti-phyA monoclonal antibody. Compared to a SDS sample buffer eluant from a column with GST alone, the GST–UBA column substantially enriched a smear of higher-molecular-mass Ub–phyA species (Figure 2b). Unmodified phyA was also present, probably due to its heterodimerization with ubiquitylated forms. Some non-modified phyA was also present in the control eluant from a column with GST alone, thus highlighting the need for a second affinity step prior to MS analysis.

Following UBA chromatography, the 8 M urea eluant was subjected to Ni–NTA chromatography using 400 mM imidazole in 8 M urea for elution. Ni–NTA eluants prepared with wild-type plants contained little protein and undetectable amounts of ubiquitylated species, as revealed by silver staining and immunoblot analyses with anti-Ub and anti-5His antibodies, respectively (Figure 2a). In contrast, a smear of Ub conjugates was evident from samples prepared with *6His-UBQ* plants. The majority of these species migrated during SDS–PAGE with apparent molecular masses greater than 90 kDa, suggesting that they represent proteins that are modified by varying-length Ub polymers.

MS analysis of Ub conjugates

Following tandem purification, the Ub conjugates were carbamido-methylated under conditions that favor cysteine modification over lysine modification (J. Peng, Emory University School of Medicine, unpublished results), and digested using trypsin. The resulting peptides were then analyzed by MudPIT MS, which separated the complex mixture by cation exchange followed by reverse-phase chromatography (Wolters *et al.*, 2001), and then analyzed the peptides by online ESI ion-trap MS (Washburn *et al.*, 2001). The masses obtained from MS/MS fragmentations were checked against the *A. thaliana* ecotype Col-0

NIH-PA Author Manuscript

NIH-PA Author Manuscript

NIH-PA Author Manuscript

protein database (version 7; http://www.Arabidopsis.org) using the SEQUEST search engine (Eng *et al.*, 1994) within the Xcalibur program to identify the parent polypeptides. A likely Ub conjugate was included in the final list if two or more peptides were identified by MS/MS with X_{corr} stringency scores greater than 2.0, 2.2 and 3.75 for the +1, +2 and +3 charge states, respectively (Peng *et al.*, 2003), and P(pro) probability scores less than 5×10^{-2} (all calculated within SEQUEST). If only a single peptide was identified (without a Ub footprint), we increased the P(pro) stringency threshold to 1.0×10^{-4} before inclusion. Inclusion of the P(pro) criterion increased the stringency as compared to previous studies (Peng *et al.*, 2003; Maor *et al.*, 2007) to help eliminate false positives. We also generated probability scores for some proteins using the MASCOT algorithm to allow direct comparison of our data to those obtained by Manzano *et al.* (2008); all but two of our MASCOT scores were more stringent than their most stringent representative, which had a score of 24 (Tables 1 and 2).

Not surprisingly, the dominant peptides in our MS/MS sequencing events were derived from Ub, and were subsequently filtered from the analyses. To help remove additional contaminants, we also performed the same analysis with samples prepared from wild-type plants subjected to both GST–UBA and Ni–NTA chromatography. The few proteins identified in these samples were omitted from the final list, although it remains possible that they are ubiquitylation targets (Table S1). Several contain one or two polymeric histidine motifs (e.g. urease accessory protein and La-containing protein), suggesting that they naturally bind to immobilized nickel.

Initial trials from several MudPIT MS analyses using young green Arabidopsis seedlings identified 44 non-redundant candidate ubiquitylated proteins. Because a number of the peptides identified matched several isoforms of the same protein, a total of 77 targets were possible (e.g. the a, d and e isoforms of cell-division-cycle-48 (CDC48); Table 1). None of the proteins on the list are confined to the internal space of the chloroplast or mitochondrion, which are not *a priori* ubiquitylome candidates, thus supporting the stringency of the enrichment method. Notably, this list includes several proteins whose half lives were predicted by genetic studies to be controlled by ubiquitylation, such as EIN3 (Binder *et al.*, 2007) and JAZ6 (Katsir *et al.*, 2008), or that are known to be short lived in plants (e.g. phenyalanine ammonia lyase; Lamb *et al.*, 1979). We also found orthologs to a set of yeast and mammalian proteins that have previously been reported to be ubiquitylated by MS/MS analysis or direct biochemical assays, including several ribosomal subunits, elongation factor 1α (EF1α), and the heat-shock proteins HSP70 and HSP81 (Peng *et al.*, 2003; Mayor and Deshaies, 2005; Denis *et al.*, 2007). Like the yeast studies, we also identified several proteins in the UPS; included in our list were CDC48, the E3 ligase UPL2, the 26S proteasome subunit RPN1a, and the de-ubiquitylating enzyme UBP12/13. Finally, we obtained a set of proteins whose modification by ubiquitylation had not previously been recorded, including Diminuto-1 and the IAA-alanine resistance protein-1 precursor.

Detection of Ub attachment sites

A key feature of the MS/MS approach is the ability to detect potential Ub attachment sites in the spectra of trypsin digests as a Ub footprint, consisting of a missed lysine cleavage in the peptide, together with a lysine residue increased in mass by two glycines (114 kDa) (Figure 3a). To confirm our ability to detect Ub footprints, we synthesized a bifurcated peptide resembling an internal fragment of Ub (residues 43–55) modified at Lys48 with the five C-terminal residues of a second Ub moiety (Figure 3b). MS analysis following extended trypsinization detected only a 1460.8 Da peptide, reflecting a single cleavage between Arg73 and Gly74 of the short extension, and found no evidence for cleavage after Lys48 of the main chain. MS/MS analysis further identified the Ub footprint in this peptide as a 242.1

NIH-PA Author Manuscript

NIH-PA Author Manuscript

NIH-PA Author Manuscript

Da separation between the y6 and y7 ions, which corresponds to the loss of an isopeptide-linked Lys-Gly-Gly sequence between the peptide fragments (Figure 3c).

When our database of MS/MS spectra was analyzed for peptides containing a lysine that was not cleaved by trypsin and was conjugated to di-glycine (increased mass of 114 Da), we identified 10 proteins with a Ub footprint, seven of which were new ubiquitylation candidates (Table 2). In two cases (histone H1.2 and EF1α), two Ub attachment sites were found. Whereas the ubiquitylation sites on histone H1.2 at Lys 156 and Lys165 were detected separately in two different peptides (Figure S2), the two on EF1α (Lys438 and Lys441) were detected in the same peptide, implying that EF1α can be ubiquitylated simultaneously at two sites. It was reported recently that trypsin can still attack lysines modified with Ub, thus questioning missed trypsin cleavage as a criterion for identifying Ub footprints (Denis *et al.*, 2007). When this caveat was used to re-search the MS/MS dataset, three additional proteins with potential Ub footprints were identified (cytochrome P450 71B7, patellin-1 and DNA methyltransferase 2; Table 2). In total, 15 Ub footprints on 13 targets were identified (Table 2). Combined with the collection identified without a Ub footprint (Table 1), our MS analyses detected 54 non-redundant ubiquitylation targets collectively expressed in Arabidopsis as 90 possible isoforms.

Ubiquitylation sites on Ub

Previous MS/MS analysis of Ub conjugates from Arabidopsis suspension cells purified by only a Ub-binding column (UBA or UIM) detected a number of peptides from Ub itself that contained Ub footprints (Maor *et al.*, 2007). In total, five of the seven lysines were found to be modified, with the order of abundance being Lys48 ≫ Lys63 > Lys11 ≫ Lys33 > Lys29. Here, we confirmed this result, and identified Lys6 as another Ub linkage site (Figure 4, Table 2 and Figure S1). In addition, we found a Ub peptide with two Ub footprints at Lys29 and Lys33 (Figure 4d). An identical di-ubiquitylated peptide was detected in yeast (Peng *et al.*, 2003; Tagwerker *et al.*, 2006), which, taken together with the results of our study, provides evidence that branched mixed-linkage Ub chains are assembled *in vivo*. The relative abundance of each Ub footprint (Table 3) matched reasonably well with the prior Arabidopsis study (Maor *et al.*, 2007), with subtle differences probably reflecting the preferences of the Ub-binding domains and the various purification strategies employed.

DISCUSSION

Comprehensive analysis of the plant ubiquitylome clearly requires stringent methods to purify Ub conjugates and then identify the targets in these complex mixtures. While MudPIT MS approaches have shown great promise in plants, as in animals, a major limitation is the ability to adequately enrich for ubiquitylated species beforehand. Challenges with plants include the sheer number of possible Ub conjugates, their diverse array of Ub linkages, their low abundance, and their instability following extraction. While single-step purifications using Ub-binding domains have shown promise (Maor *et al.*, 2007; Manzano *et al.*, 2008), we found that additional steps(s) are necessary to avoid contamination with non-ubiquitylated species and proteins that non-covalently interact with Ub or the column matrix.

Our strategy combines tandem Ub-affinity and Ni–NTA purification steps with use of a transgenic Arabidopsis line expressing high levels of 6xHis-tagged Ub. Prior studies demonstrated that 6xHis-tagged Ub can be readily incorporated into Ub conjugates in yeast and animals, and appears to be biologically equivalent to wild-type Ub in yeast (Ling *et al.*, 2000; Peng *et al.*, 2003; Kirkpatrick *et al.*, 2005; Mayor *et al.*, 2005). While this functional similarity has not yet been unequivocally demonstrated in plants, we and others have shown that 6xHis-tagged Ub can be conjugated to proteins *in planta* (Ling *et al.*, 2000 and this

NIH-PA Author Manuscript

NIH-PA Author Manuscript

NIH-PA Author Manuscript

paper). Furthermore, we found that high level expression of 6xHis-tagged Ub with a MHHHHHHGGGGGA extension does not compromise the growth and development of Arabidopsis or demonstrably interfere with the UPS. The advantages of 6xHis-tagged Ub purification include the ability to: (i) bind, wash and elute Ub conjugates under strong denaturing conditions (8 M urea), (ii) utilize a purification step that is not dependent on recognition of the Ub moiety, (iii) enrich for Ub conjugates regardless of the topological nature of bound Ubs (mono-versus poly-ubiquitylation at various internal lysines), and (iv) re-use of the matrix. Here, we employed a UBA domain for the first enrichment step. As this domain preferentially binds poly-ubiquitylated proteins bearing Lys48-linked Ub chains (a conclusion supported by our MS analysis of Ub linkages; Table 3), the final preparations were probably enriched in proteins awaiting degradation by the UPS. In the future, other Ub-binding domains [e.g. UIM, p62, pleckstrin, motif interacting with Ub (MIU) and ZnF-UBP domains (Harper and Schulman, 2006; Schreiner *et al.*, 2008)] could also be exploited for the first enrichment step. Because some prefer Ub monomers or Ub polymers internally linked through other Ub lysines (e.g. Lys6 and Lys63), it may be possible to obtain subsets of Ub conjugates (Mayor *et al.*, 2007), and thus focus on other processes regulated by ubiquitylation (e.g. vesicular trafficking, chromatin remodeling or DNA repair).

Although the prior method described by Ling *et al.* (2000) showed poor recovery of 6xHis-tagged Ub conjugates by Ni–NTA chromatography, our new tag offered increased yield. A possible reason is our extension of the 6xHis tag further beyond the Ub moiety to improve access to the Ni–NTA resin. Another reason could be the increased incorporation of 6xHis-tagged Ub into Ub–protein conjugates, which was achieved by higher expression of the tagged Ub relative to the endogenous pool of wild-type Ub. The optimal situation would be complete replacement of wild-type Ub with the tagged variant as has been done in yeast (Peng *et al.*, 2003). Unfortunately, this approach is impractical in plants where Ub is encoded by large gene families (e.g. 14 *UBQ* coding genes in *A. thaliana*; Callis *et al.*, 1995). As an alternative, we created a transgene expressing a polymeric Ub chain tandemly expressing six 6xHis-tagged Ub moieties that exploited the activities of endogenous de-ubiquitylating enzymes to release Ub monomers. Previous studies with a range of engineered Ub fusions imply that these de-ubiquitylating enzymes can readily process such synthetic translationally linked Ub polymers *in planta* (Hondred *et al.*, 1999; Walker and Vierstra, 2007).

We attempted to further increase the 6xHis-tagged Ub/Ub ratio by combining the *6His-UBQ* transgene with T-DNA insertion mutants disrupting two of the highest expressed poly-*UBQ* genes, *UBQ3* and *UBQ10*. Unfortunately, neither transgene/mutant combination improved the ratio (data not shown). One reason could be that disruption of these two *UBQ* genes by themselves is insufficient to reduce the Ub pool. As transcription of the poly-*UBQ* gene *UBI4* in yeast appears to be feedback-regulated by Ub availability (Swaminathan *et al.*, 1999; London *et al.*, 2004; Hanna *et al.*, 2007), another possible reason is that expression of the remaining endogenous Arabidopsis *UBQ* genes is up-regulated upon inactivation of *UBQ3* and *UBQ10*. Several of our *6His-UBQ* transgenic lines showed a gradual and sometimes rapid decline in the levels of free 6xHis-tagged Ub in subsequent generations. We presume that this attenuation reflects epigenetic silencing of the transgene by the native *UBQ* loci (Becker *et al.*, 1993). Consequently, care must be taken to select for stable, high-expression lines during seed propagation and after introgression of the *6His-UBQ* transgene into various mutant backgrounds.

One approach to increase the yield of Ub conjugates on Ni–NTA columns is to exploit a K48R variant that terminates poly-ubiquitylation (Ling *et al.*, 2000). Our strategy deliberately avoided this mutation, given its potential to slow Ub conjugate turnover by either shortening the length of the Ub chain or interfering with its recognition by Ub

NIH-PA Author Manuscript

NIH-PA Author Manuscript

NIH-PA Author Manuscript

receptors. Collectively, these effects could artifactually alter the pool of native Ub conjugates. Previous studies showing that high-level expression of K48R or K63R Ub substantially compromises plant growth illustrate the risk (Bachmair *et al.*, 1990; Becker *et al.*, 1993; Schlogelhofer *et al.*, 2006; Yin *et al.*, 2007).

Although the tandem affinity strategy appears to be an improvement over current single-step methods, we acknowledge that the protocol still requires optimization. While approximately 50% of the immunodetectable Ub conjugates in crude extracts could be enriched by the GST–UBA step, only approximately 5% were retained and eluted from the Ni–NTA column. Most Ub conjugates did not bind, suggesting that: (i) accessibility of the 6xHis tag to the Ni–NTA resin requires improvement, (ii) increased incorporation of 6xHis-tagged Ub into conjugates is required, and/or (iii) improved conditions are needed to bind the 6xHis-tagged Ub moieties to the chelated nickel.

Our list of ubiquitylated proteins further extends the ubiquitylome in plants beyond the attempts described recently (Maor *et al.*, 2007; Manzano *et al.*, 2008). The three lists show little overlap both in terms of protein detection and Ub footprints (see Tables 1 and 2), implying that the current collective coverage is far from complete. The list presented here is significantly enriched (26 of 54 candidates) in proteins that were previously expected to be targets of ubiquitylation, either by genetic analyses, reports of a short-half life, or by comparison with initial descriptions of the yeast and animal ubiquitylomes. While this preponderance suggests that the tandem UBA/Ni–NTA purification strategy more effectively purifies ubiquitylated proteins compared to the single-step methods, more exhaustive MS/MS analyses are required to confirm this possibility. It should also be noted that a number of prominent ubiquitylation targets are conspicuously absent from our and previous lists (this paper; Manzano *et al.*, 2008; Maor *et al.*, 2007), including AUX/IAA proteins, histone H2B, ABI5 and phyA. Some omissions may reflect the low abundance or rapid turnover of these ubiquitylated species (AUX/IAA proteins), proteins with Ub topology that does not interact well with UBA domains (mono-ubiquitylated histone H2B), the lack of depth in the MS analysis, or the analysis of Arabidopsis tissues where these targets are not abundant (ABI5 and phyA). As with previous MS/MS studies with Arabidopsis (Maor *et al.*, 2007) and other organisms (Hitchcock *et al.*, 2003; Peng *et al.*, 2003; Mayor *et al.*, 2005), we detected potential Ub attachment sites for several proteins. We also found little sequence consensus adjacent to the modified lysine (Table 2), implying that the residues surrounding the Ub-binding site are not important determinants for ubiquitylation, except that the region must be solvent-exposed.

Several ubiquitylated proteins listed here deserve discussion. EIN3 and JAZ6 have been shown to be key regulators of ethylene and jasmonic acid perception, with their turnover helping to restrain signaling in the absence of the hormone and dampen continued signaling afterwards. EIN3 and JAZ6 turnover has been inferred to be directed by Ub ligation through genetic analyses (Binder *et al.*, 2007; Katsir *et al.*, 2008), and our study confirms that they are indeed ubiquitylated. Although the core histone H2B has been demonstrated to be reversibly ubiquitylated in Arabidopsis as it is in other eukaryotes (Fleury *et al.*, 2007; Liu *et al.*, 2007; Sridhar *et al.*, 2007), little is currently known about ubiquitylation of the linker histone H1. Our MS/MS sequence analyses identified two linkage sites in the H1.2 isoform, involving Lys156 and Lys165 (Table 2 and Figure 2a,b). Mice and humans also ubiquitylate histone H1, with the attachment site in the mouse protein being very close to that of its Arabidopsis counterpart (Figure S2c) (Wang *et al.*, 2002; Wisniewski *et al.*, 2007). In *Drosophila*, this modification appears to require TAF120, a conserved subunit of the TFIID transcription factor complex, which uniquely contains both Ub-activating enzyme (E1)- and Ub-conjugating enzyme (E2)-type activities (Pham and Sauer, 2000). A potential Arabidopsis ortholog of TAF120 exists that could direct this modification.

NIH-PA Author Manuscript

NIH-PA Author Manuscript

NIH-PA Author Manuscript

Our list is notably enriched for proteins within the UPS (CDC48, the E3 ligase UPL2, the 26S proteasome subunit RPN1a, and the de-ubiquitylating enzyme UBP12/13), involved in translation (ribosomal subunits L7a, L8 and S3, the translation initiation factor eIF-1A, and EF1α), and/or membrane-associated (VAMP7B and patellin-1). Given the harsh conditions used for the Ni–NTA chromatography, it is unlikely that the UPS components were isolated based on their non-covalent affinity for Ub bound to other proteins, implying that they are also ubiquitylated. One example is CDC48, which has a central role in the UPS-dependent turnover of misfolded ER-resident proteins after their retrograde transport back to the cytosol (Bar-Nun, 2005) and was reported to be ubiquitylated in yeast (Hitchcock *et al.*, 2003; Peng *et al.*, 2003). Evidence for ribosomal subunits being ubiquitylated has been presented previously for both Arabidopsis and yeast (Mayor *et al.*, 2005; Tagwerker *et al.*, 2006; Maor *et al.*, 2007; Kraft *et al.*, 2008). This modification could represent a regulatory step during ribosome assembly and/or translation, or implicate the UPS in the removal of improperly folded subunits or entire ribosomes when they become non-functional or less important upon cell starvation (Kraft *et al.*, 2008). The preponderance of membrane-associated proteins is in agreement with the first analysis of the entire yeast ubiquitylome (Peng *et al.*, 2003), and was supported by subsequent MS analysis of ubiquitylated ER proteins (Hitchcock *et al.*, 2003). Collectively, it could further emphasize the importance of ubiquitylation and the UPS in the catabolism and trafficking of membrane-associated proteins.

Our data, combined with those of Maor *et al.* (2007), provide strong evidence that multiple types of polymeric Ub chains are assembled in plants. In fact, we found that all lysines except Lys27 are used as concatenation sites for additional Ubs. While it remains possible that Lys27 can be ubiquitylated but that these footprints escape MS detection, a more likely reason is that because of its epsilon amino group is not solvent-exposed it is inaccessible to Ub–protein ligases (Figure 4a). Of the total of 397 Ub–Ub linkages detected here, we found only one obvious MS spectrum diagnostic for the Lys63 linkage, compared to 354 for the Lys48 linkage (Figure S1 and Table 3). Enrichment for Lys48 chains agrees with the preference of RAD23 (HHR23A) for Lys48-linked poly-Ub chains (Raasi and Pickart, 2003; Raasi *et al.*, 2004). The paucity of Lys63 linkages observed here also suggests that mixed Ub polymers bearing both Lys63 and Lys48 chains are not synthesized *in vivo*. A substantially higher percentage of Lys63 chains was detected after the single Ub-affinity purification by Maor *et al.* (2007), which could reflect the different affinities of the Ub-binding domains used for purification (UBA domains from AtUBP14 or HHR23A), or differences between the tissue types examined (suspension cells versus whole seedlings). In addition, we found evidence for a single Ub moiety simultaneously serving as the concatenation site for two Ubs via Lys29 and Lys33. This raises the possibility that highly complex mixed-linkage Ub chains exist involving any combination of the six Ub lysines. If so, ubiquitylation could approach the complexity of protein glycosylation in forming a multitude of branched polymers, each having their own functions and receptors. The first proof of this possibility was the demonstration that such topologically complex polymers can be assembled on a single substrate *in vitro* (Kirkpatrick *et al.*, 2006).

While our list represents only a small fraction of the complete Arabidopsis ubiquitylome, it is an important first step in understanding the extent of Ub conjugation in an intact untreated plant. In addition to further optimization of the tagged Ub, its incorporation into conjugates, and enrichment of the ubiquitylated species by alternative Ub-binding reagents, we now hope to improve the depth of coverage by using of the next generation of mass spectrometers with higher sensitivities, speeds and mass accuracies (e.g. linear trap quadrupole mass spectrometers).

NIH-PA Author Manuscript
NIH-PA Author Manuscript
NIH-PA Author Manuscript

EXPERIMENTAL PROCEDURES

Creation of plants expressing 6xHis-tagged Ub

The *6His-UBQ* transgene was assembled using the third Ub coding region in *AtUBQ11* (At4g05050; Callis *et al.*, 1995) present in the plasmid p6169 (L.R. Ling and J. Callis, Department of Molecular and Cellular Biology, University of California-Davis, unpublished results). The start codon was mutated to encode an alanine residue (GCG) by Quikchange site-directed mutagenesis (Stratagene, http://www.stratagene.com/). This plasmid was then cut with *Nde*I to insert a double-stranded linker TATGCATCACCATCACCATCACGGTGGAGGAGGTTCAGCGCA that encoded an N-terminal extension of MHHHHHHGGGGGSA, with the alanine residue representing the location of the original start methionine.

The 5′ or 3′ ends of this *6His-Gly-UBQ* fragment were then mutated to contain various restriction sites by PCR, inserted into pBSKS (Stratagene), digested with the appropriate restriction enzymes, and then connected sequentially to generate a poly-*UBQ* gene expressing six tandem Ub repeats. Coding region pSS31 was generated with *Xba*I and *Nde*I sites at the 5′ end and a *Sph*I site at the 3′ end by PCR using primer 1 (5′-GTTCTAGACATATGCATCACCATCACCAT-3′) and primer 2 (5′-ATGCATGCCACCACGGAGACGGAG-3′). The coding frame pSS32 was generated with an *Sph*I site at the 5′ end, and an *Ase*I site, a stop codon, an *Nhe*I site and a *Kpn*I site at the 3′ end by PCR using primer 3 (5′-GTGCATGCATCACCATCACCAT-3′) and primer 4 (5′-ACTCTAGAGCTAGCTCAATTAATGCCACCACGGAGACGGAG-3′). Coding frame pSS33 was generated with *Sph*I sites at the 5′ and 3′ ends by PCR amplification with primers 2 and 3. Sequence-verified and digested fragments pSS31 and pSS32 were ligated to create the di-*UBQ* coding region pSS34. This plasmid was then cut with *Sph*I and ligated with a similarly digested pSS33 fragment to create the tri-*UBQ* coding region pSS35. To create the hexa-*UBQ* coding region, the *Xba*I/*Ase*I-digested *UBQ* fragment from pSS35 was ligated into *Nde*I/*Xba*I-digested pSS35 to create pSS36, with six tandem *6His-UBQ* coding frames followed by a stop codon. pSS36 was then cut with *Xba*I/*Nhe*I and ligated into *Xba*I-digested pGSVE9 (E. Babiychuk and S. Kushnir, Department of Plant Systems Biology, Flanders Institute of Biotechnology, Belgium, unpublished results) between the CaMV *35S* promoter and the *Agrobacterium tumefaciens nopaline synthase* (*NOS*) 3′ untranslated region.

The *6His-UBQ* transgene was introduced into *A. tumefaciens* and then into *A. thaliana* ecotype Columbia-0 (Col-0) via the floral-dip method as described previously (Clough, 2005). Transformants were selected on the basis of hygromycin B resistance (Sigma, http://www.sigmaaldrich.com/) and by immunoblot detection of 6xHis-tagged Ub using anti-Ub antibodies.

Plant growth conditions and phenotypic analyses

Arabidopsis thaliana ecotype Col-0 seeds were stratified for 3 days at 4°C in the dark and then sown in liquid Gamborg's B-5 medium (GM) (Sigma) containing 2% sucrose and 0.5 g/l 4-morpholineethanesulfonic acid (MOPS), with the pH of the medium adjusted to 5.7 using KOH. Solid GM contained 0.7% agar.

phyA degradation was analyzed using 5-day-old etiolated seedlings exposed to 142 μmol m^{-2} sec^{-1} red light (660 nm) provided by light-emitting diodes. ABI5 levels were assessed in light-grown seedlings grown for 5 days in liquid GM medium and then exposed for various times to 50 μ_M ABA (Sigma). Crude extracts were subjected to SDS–PAGE and immunoblot analysis using a monoclonal antibody against oat phyA (Oat-22; Cordonnier *et al.*, 1985) or polyclonal anti-ABI5 antibodies (Stone *et al.*, 2006) in conjunction with

NIH-PA Author Manuscript

NIH-PA Author Manuscript

NIH-PA Author Manuscript

appropriate horseradish peroxidase-conjugated secondary antibodies (KPL, http://www.kpl.com). Trichomes were examined on the first true leaf of 14-day-old wild-type and *6His-UBQ* plants grown on solid GM under continuous white light. For root elongation, seeds were germinated on solid GM for 5 days under a long-day photoperiod (16 h light/8 h dark). The plants were then transferred to solid GM medium containing various amounts of canavanine (Sigma), *p*-fluorophenylalanine (Sigma) or MG132 (Biomol, http://www.biomol.com) and grown vertically for an additional 7 days.

Preparation of UBA-affinity beads

A plasmid encoding the UBA1 and 2 domains of human HHR23A protein fused to the C-terminus of GST (Raasi and Pickart, 2003) was obtained from S. Rassi and C. Pickart (Department of Biochemistry, Johns Hopkins University). The GST–UBA protein was expressed in BL21 pLysS *Escherichia coli*, purified by glutathione Sepharose 4B chromatography (GE Biosciences, http://www.gehealthcare.com), and dialyzed overnight against 50 mM MOPS (pH 7.5). The protein was coupled to Affi-Gel 15 (Bio-Rad, http://www.bio-rad.com/) overnight at 4°C at a concentration of 15 mg ml^{-1}. The coupled beads were quenched using 100 mM Tris/HCl (pH 7.5), washed with 10 volumes of MOPS, followed by 10 volumes of extraction buffer (EB: 200 mM NaCl, 25 mM Tris/HCl pH 7.2 and 0.25% Triton X-100), and finally with 10 volumes of EB plus 2 M NaCl, and then stored at 4°C in EB.

Purification of Ub–protein conjugates

Wild-type and *6His-UBQ* plants were grown for 10 days under continuous light at 26°C in liquid GM, harvested and blotted dry, rapidly frozen in liquid nitrogen, and then stored at −80°C until use. Frozen tissue (approximately 100 g) was pulverized at the temperature of liquid nitrogen, and then mixed with 0.5 g ml^{-1} EB containing freshly added 1× protease inhibitor cocktail (Roche, http://www.roche.com), 2 mM phenylmethanesulfonyl fluoride, 10 mM iodoacetamide and 10 mM sodium metabisulfite. Unless noted, all subsequent manipulations were performed at 4°C. The homogenate was filtered through two layers of Miracloth (EMD Biosciences, http://www.emdbiosciences.com) and clarified at 27 000 ***g*** for 20 min.

Homogenates equivalent to 20 g of tissue were gently mixed with 500 μl of the GST–UBA beads for 1.5 h at 4°C, collected by centrifugation at 500 ***g*** for 5 min, and washed three times with EB and twice with EB plus 2 M NaCl. Bound proteins were eluted with 2 ml urea buffer (8 M urea, 100 mM NaH_2PO_4, 10 mM Tris/HCl pH 8.0) at room temperature. Imidazole and iodoacetamide were added to final concentrations of 20 and 10 mM, respectively, and the eluant was incubated for 1 h with 100 μl of Ni–NTA agarose (Qiagen, http://www.qiagen.com/) pre-equilibrated in the same buffer. After collection by centrifugation at 500 ***g*** for 5 min, the beads were washed once in urea buffer plus 0.5% SDS, twice in urea buffer plus 0.5% Triton X-100 and 20 mM imidazole, and three times in urea buffer. Bound proteins were eluted with 400 mM imidazole in urea buffer. Multiple eluants were pooled and concentrated using a 10 kDa molecular weight cut-off Microcon concentrator (Millipore, http://www.millipore.com). After SDS–PAGE, 6xHis-tagged Ub conjugates were detected by immunoblot analysis with anti-Ub (Smalle *et al.*, 2003) and anti-5His (Novagen, http://www.emdbiosciences.com) antibodies.

Mass spectrometry

Ubiquitylated protein mixtures (100 μl) were carbamidomethylated in the dark by reduction with 10 mM DTT, followed by alkylation with 30 mM iodoacetamide for 1 h, and quenching of the iodoacetamide with 20 μl of 200 mM DTT for 1 h. The reaction mixture was kept at room temperature to minimize the addition of acetamide groups to lysine residues (Nielsen

NIH-PA Author Manuscript

NIH-PA Author Manuscript

NIH-PA Author Manuscript

et al., 2008; J. Peng, Emory University School of Medicine, unpublished results). Samples were diluted 10-fold with 25 mM ammonium bicarbonate, and incubated at 37°C for 12 h with 2 μg trypsin (Trypsin Gold, mass spectrometry grade, Promega, http://www.promega.com/) followed by a second 6 h incubation with an additional 2 μg of trypsin. A synthetic peptide corresponding to the five C-terminal residues of Ub (RLRGG) linked at Lys48 via an isopeptide bond to the internal Ub fragment (LIF-AGKQLEDGR) (see Figure 3b) was synthesized by the University of Wisconsin Peptide Synthesis Facility, and purified to 98% by preparative HPLC. This peptide was trypsinized as above before MS analysis.

Trypsin digests were desalted using a C18 solid-phase extraction pipette tip (SPEC PT C18, Varian Inc., http://www.varianinc.com), vacuum-dried, and reconstituted in 20 μl of 95% H_2O, 5% acetonitrile and 0.1% formic acid. The desalted trypsin digests were then loaded on a fused-silica microcapillary column and subjected to MudPIT MS analysis (Washburn *et al.*, 2001; Wolters *et al.*, 2001), involving a μHPLC system connected to an ESI ion-trap mass spectrometer (Surveyor HPLC and LCQ deca XPplus, ThermoElectron, http://www.michrom.com). The HPLC separation utilized a fused-silica, fritless microcapillary column (100 μm inside diameter, 365 μm outside diameter) packed with 10 cm of C18 resin (Magic C18, Michrom Bioresources Inc., http://www.michrom.com) followed by 3 cm of cation-exchange (SCX) resin (polysulfoethy A, Western Analytical Products Inc., http://www.westernanalytical. com). The tip at the end of the fused-silica capillary was pulled using a P-2000 laser puller (Sutter Instruments Co., http://www.sutter.com). The capillary column was connected to the HPLC through a PEEK microcross, with a platinum wire inserted into the flow-through to supply a spray voltage of 1.8 kV. Six separate salt-elution steps (0, 25, 62.5, 125, 200 and 500 mM ammonium acetate, pH 7.0) were performed for 2 min each, each followed by a 5–95% acetonitrile reverse-phase gradient in 0.1% formic acid at a flow rate of 300 nl min^{-1}. Each reverse-phase step began with 5% acetonitrile for 25 min, a gradient of 5–35% acetonitrile over 150 min, 35–65% acetonitrile over 60 min, and then 65–95% acetonitrile over 10 min. The ion-trap mass spectrometer was set up to run in 'biggest 3' mode. A full-mass scan was performed between *m/z* 400 and 1500, followed by three MS/MS scans of the three highest-intensity parent ions at 45% relative collision energy. Dynamic exclusion was enabled, with a repeat count of 3, an exclusion duration of 1 min, and a repeat duration of 20 min.

Mass spectrometry data analysis

The acquired MS/MS spectra were searched against the *A. thaliana* Col-0 protein database (TAIR7 genome release of 23 April 2007) using the SEQUEST program (ThermoFinnigan, http://www.thermo.com) (Eng *et al.*, 1994). Sequences for 6xHis-tagged Ub, GST–UBA, trypsin and major human keratin were included in the database to decrease the false-positive rate. Masses for both precursor and fragment ions were treated as mono-isotopic. The mass shift of 114.1 Da for lysine residues was included as a variable modification to determine ubiquitylation sites. Oxidized methionine (+16 Da) and carbamidomethylated cysteines (+57 Da) were also set as variable modifications. The initial search was set to allow for up to two missed trypsin cleavages at ubiquitylated lysines (Figure 3) (Peng *et al.*, 2003), with a follow-up data analysis that permitted this cleavage (Denis *et al.*, 2007).

Supplementary Material

Refer to Web version on PubMed Central for supplementary material.

NIH-PA Author Manuscript

NIH-PA Author Manuscript

NIH-PA Author Manuscript

Acknowledgments

This work was supported by grants from the National Science Foundation Arabidopsis 2010 Program (MCB-0115870) and the University of Wisconsin College of Agricultural and Life Sciences (to R.D.V.), a National Heart, Lung, and Blood Institute Proteomics Center Contract N01-HV-28182 (to L.M.S. and M.S.), and a post-doctoral fellowship from the WennerGren Foundation, Sweden (to M.H.). We thank Drs Cecile Pickart and Sharhi Raasi (Department of Biochemistry, Johns Hopkins University) for the *GST–UBA* expression plasmid.

References

Bachmair A, Becker F, Masterson RV, Schell J. Perturbation of the ubiquitin system causes leaf curling, vascular tissue alterations and necrotic lesions in a higher plant. EMBO J. 1990; 9:4543–4549. [PubMed: 2176155]

Bar-Nun S. The role of p97/Cdc48p in endoplasmic reticulum-associated degradation: from the immune system to yeast. Curr Top Microbiol Immunol. 2005; 300:95–125. [PubMed: 16573238]

Becker F, Buschfeld E, Schell J, Bachmair A. Altered response to viral infection by tobacco plants perturbed in ubiquitin system. Plant J. 1993; 3:875–881.

Binder BM, Walker JM, Gagne JM, Emborg TJ, Hemmann G, Bleecker AB, Vierstra RD. The Arabidopsis EIN3 binding F-box proteins EBF1 and EBF2 have distinct but overlapping roles in ethylene signaling. Plant Cell. 2007; 19:509–523. [PubMed: 17307926]

Book AJ, Smalle J, Lee KH, et al. The RPN5 subunit of the 26S proteasome is essential for gametogenesis, sporophyte development, and complex assembly in Arabidopsis. Plant Cell. 2009; 21:460–478. [PubMed: 19252082]

Callis J, Carpenter T, Sun CW, Vierstra RD. Structure and evolution of genes encoding polyubiquitin and ubiquitin-like proteins in *Arabidopsis thaliana* ecotype Columbia. Genetics. 1995; 139:921–939. [PubMed: 7713442]

Clough SJ. Floral dip: *Agrobacterium*-mediated germ line transformation. Methods Mol Biol. 2005; 286:91–102. [PubMed: 15310915]

Clough RC, Jordan-Beebe ET, Lohman KN, Marita JM, Walker JM, Gatz C, Vierstra RD. Sequences within both the N- and C-terminal domains of phytochrome A are required for Pfr ubiquitination and degradation. Plant J. 1999; 17:155–167. [PubMed: 10074713]

Cordonnier MM, Greppin H, Pratt LH. Monoclonal antibodies with differing affinities to the red-absorbing and far-red-absorbing forms of phytochrome. Biochemistry. 1985; 24:3246–3253.

Denis NJ, Vasilescu J, Lambert JP, Smith JC, Figeys D. Tryptic digestion of ubiquitin standards reveals an improved strategy for identifying ubiquitinated proteins by mass spectrometry. Proteomics. 2007; 7:868–874. [PubMed: 17370265]

Doelling JH, Yan N, Kurepa J, Walker J, Vierstra RD. The ubiquitin-specific protease UBP14 is essential for early embryo development in *Arabidopsis thaliana*. Plant J. 2001; 27:393–405. [PubMed: 11576424]

Downes BP, Stupar RM, Gingerich DJ, Vierstra RD. The HECT ubiquitin-protein ligase (UPL) family in Arabidopsis: UPL3 has a specific role in trichome development. Plant J. 2003; 35:729–742. [PubMed: 12969426]

Dreher K, Callis J. Ubiquitin, hormones and biotic stress in plants. Ann Bot. 2007; 99:787–822. [PubMed: 17220175]

Eng JK, McCormack AL, Yates JR III. An approach to correlate tandem mass spectral data of peptides with amino acid sequences in a protein database. J Am Soc Mass Spectrom. 1994; 5:976–989.

Fleury D, Himanen K, Cnops G, et al. The *Arabidopsis thaliana* homolog of yeast BRE1 has a function in cell cycle regulation during early leaf and root growth. Plant Cell. 2007; 19:417–432. [PubMed: 17329565]

Hanna J, Meides A, Zhang DP, Finley D. A ubiquitin stress response induces altered proteasome composition. Cell. 2007; 129:747–759. [PubMed: 17512408]

Harper JW, Schulman BA. Structural complexity in ubiquitin recognition. Cell. 2006; 124:1133–1136. [PubMed: 16564007]

NIH-PA Author Manuscript

NIH-PA Author Manuscript

NIH-PA Author Manuscript

Hitchcock AL, Auld K, Gygi SP, Silver PA. A subset of membrane-associated proteins is ubiquitinated in response to mutations in the endoplasmic reticulum degradation machinery. Proc Natl Acad Sci USA. 2003; 100:12735–12740. [PubMed: 14557538]

Hondred D, Walker JM, Matthew D, Vierstra RD. Use of ubiquitin fusions to augment protein expression in transgenic plants. Plant Physiol. 1999; 119:713–724. [PubMed: 9952468]

Jang S, Marchal V, Panigrahi KC, Wenkel S, Soppe W, Deng XW, Valverde F, Coupland G. Arabidopsis COP1 shapes the temporal pattern of CO accumulation conferring a photoperiodic flowering response. EMBO J. 2008; 27:1277–1288. [PubMed: 18388858]

Katsir L, Schilmiller AL, Staswick PE, He SY, Howe GA. COI1 is a critical component of a receptor for jasmonate and the bacterial virulence factor coronatine. Proc Natl Acad Sci USA. 2008; 105:7100–7105. [PubMed: 18458331]

Kirkpatrick DS, Weldon SF, Tsaprailis G, Liebler DC, Gandolfi AJ. Proteomic identification of ubiquitinated proteins from human cells expressing His-tagged ubiquitin. Proteomics. 2005; 5:2104–2111. [PubMed: 15852347]

Kirkpatrick DS, Hathaway NA, Hanna J, Elsasser S, Rush J, Finley D, King RW, Gygi SP. Quantitative analysis of *in vitro* ubiquitinated cyclin B1 reveals complex chain topology. Nat Cell Biol. 2006; 8:700–710. [PubMed: 16799550]

Kraft C, Deplazes A, Sohrmann M, Peter M. Mature ribosomes are selectively degraded upon starvation by an autophagy pathway requiring the Ubp3p/Bre5p ubiquitin protease. Nat Cell Biol. 2008; 10:602–610. [PubMed: 18391941]

Lamb CJ, Merritt TK, Butt VS. Synthesis and removal of phenylalanine ammonia-lyase activity in illuminated discs of potato tuber parenchyme. Biochim Biophys Acta. 1979; 582:196–212. [PubMed: 760822]

Ling R, Colon E, Dahmus ME, Callis J. Histidine-tagged ubiquitin substitutes for wild-type ubiquitin in *Saccharomyces cerevisiae* and facilitates isolation and identification of *in vivo* substrates of the ubiquitin pathway. Anal Biochem. 2000; 282:54–64. [PubMed: 10860499]

Liu Y, Koornneef M, Soppe WJ. The absence of histone H2B monoubiquitination in the Arabidopsis *hub1* (*rdo4*) mutant reveals a role for chromatin remodeling in seed dormancy. Plant Cell. 2007; 19:433–444. [PubMed: 17329563]

London MK, Keck BI, Ramos PC, Dohmen RJ. Regulatory mechanisms controlling biogenesis of ubiquitin and the proteasome. FEBS Lett. 2004; 567:259–264. [PubMed: 15178333]

Manzano C, Abraham Z, Lopez-Torrejon G, Del Pozo JC. Identification of ubiquitinated proteins in Arabidopsis. Plant Mol Biol. 2008; 68:145–158. [PubMed: 18535787]

Maor R, Jones A, Nuhse TS, Studholme DJ, Peck SC, Shirasu K. Multidimensional protein identification technology (MudPIT) analysis of ubiquitinated proteins in plants. Mol Cell Proteomics. 2007; 6:601–610. [PubMed: 17272265]

Matsumoto M, Hatakeyama S, Oyamada K, Oda Y, Nishimura T, Nakayama KI. Large-scale analysis of the human ubiquitin-related proteome. Proteomics. 2005; 5:4145–4151. [PubMed: 16196087]

Mayor T, Deshaies RJ. Two-step affinity purification of multiubiquitylated proteins from *Saccharomyces cerevisiae*. Methods Enzymol. 2005; 399:385–392. [PubMed: 16338370]

Mayor T, Lipford JR, Graumann J, Smith GT, Deshaies RJ. Analysis of polyubiquitin conjugates reveals that the Rpn10 substrate receptor contributes to the turnover of multiple proteasome targets. Mol Cell Proteomics. 2005; 4:741–751. [PubMed: 15699485]

Mayor T, Graumann J, Bryan J, MacCoss MJ, Deshaies RJ. Quantitative profiling of ubiquitylated proteins reveals proteasome substrates and the substrate repertoire influenced by the Rpn10 receptor pathway. Mol Cell Proteomics. 2007; 6:1885–1895. [PubMed: 17644757]

Mukhopadhyay D, Riezman H. Proteasome-independent functions of ubiquitin in endocytosis and signaling. Science. 2007; 315:201–205. [PubMed: 17218518]

Nielsen ML, Vermeulen M, Bonaldi T, Cox J, Moroder L, Mann M. Iodoacetamide-induced artifact mimics ubiquitination in mass spectrometry. Nat Methods. 2008; 5:459–460. [PubMed: 18511913]

Peng J, Schwartz D, Elias JE, Thoreen CC, Cheng D, Marsischky G, Roelofs J, Finley D, Gygi SP. A proteomics approach to understanding protein ubiquitination. Nat Biotechnol. 2003; 21:921–926. [PubMed: 12872131]

NIH-PA Author Manuscript

NIH-PA Author Manuscript

NIH-PA Author Manuscript

Pham AD, Sauer F. Ubiquitin-activating/conjugating activity of TAFII250, a mediator of activation of gene expression in *Drosophila*. Science. 2000; 289:2357–2360. [PubMed: 11009423]

Raasi S, Pickart CM. Rad23 ubiquitin-associated domains (UBA) inhibit 26S proteasome-catalyzed proteolysis by sequestering lysine 48-linked polyubiquitin chains. J Biol Chem. 2003; 278:8951–8959. [PubMed: 12643283]

Raasi S, Orlov I, Fleming KG, Pickart CM. Binding of polyubiquitin chains to ubiquitin-associated (UBA) domains of HHR23A. J Mol Biol. 2004; 341:1367–1379. [PubMed: 15321727]

Schlogelhofer P, Garzon M, Kerzendorfer C, Nizhynska V, Bachmair A. Expression of the ubiquitin variant UbR48 decreases proteolytic activity in *Arabidopsis* and induces cell death. Planta. 2006; 223:684–697. [PubMed: 16200408]

Schreiner P, Chen X, Husnjak K, Randles L, Zhang N, Elsasser S, Finley D, Dikic I, Walters KJ, Groll M. Ubiquitin docking at the proteasome through a novel pleckstrin-homology domain interaction. Nature. 2008; 453:548–552. [PubMed: 18497827]

Smalle J, Vierstra RD. The ubiquitin 26S proteasome proteolytic pathway. Annu Rev Plant Biol. 2004; 55:555–590. [PubMed: 15377232]

Smalle J, Kurepa J, Yang P, Emborg TJ, Babiychuk E, Kushnir S, Vierstra RD. The pleiotropic role of the 26S proteasome subunit RPN10 in Arabidopsis growth and development supports a substrate-specific function in abscisic acid signaling. Plant Cell. 2003; 15:965–980. [PubMed: 12671091]

Sridhar VV, Kapoor A, Zhang K, Zhu J, Zhou T, Hasegawa PM, Bressan RA, Zhu JK. Control of DNA methylation and heterochromatic silencing by histone H2B deubiquitination. Nature. 2007; 447:735–738. [PubMed: 17554311]

Stone SL, Williams LA, Farmer LM, Vierstra RD, Callis J. KEEP ON GOING, a RING E3 ligase essential for Arabidopsis growth and development, is involved in abscisic acid signaling. Plant Cell. 2006; 18:3415–3428. [PubMed: 17194765]

Swaminathan S, Amerik AY, Hochstrasser M. The Doa4 deubiquitinating enzyme is required for ubiquitin homeostasis in yeast. Mol Biol Cell. 1999; 10:2583–2594. [PubMed: 10436014]

Tagwerker C, Flick K, Cui M, Guerrero C, Dou Y, Auer B, Baldi P, Huang L, Kaiser P. A tandem affinity tag for two-step purification under fully denaturing conditions: application in ubiquitin profiling and protein complex identification combined with *in vivo* cross-linking. Mol Cell Proteomics. 2006; 5:737–748. [PubMed: 16432255]

van Nocker S, Vierstra RD. Multiubiquitin chains linked through lysine-48 are abundant *in vivo* and competent intermediates in the ubiquitin-dependent proteolytic pathway. J Biol Chem. 1993; 268:24766–24773. [PubMed: 8227036]

Vierstra RD. The ubiquitin/26S proteasome pathway, the complex last chapter in the life of many plant proteins. Trends Plant Sci. 2003; 8:135–142. [PubMed: 12663224]

Vierstra RD. The ubiquitin/26S proteasome system at the nexus of plant biology. Nat Rev Mol Cell Biol. 2009 in press.

Vijay-Kumar S, Bugg CE, Wilkinson KD, Vierstra RD, Hatfield PM, Cook WJ. Comparison of the three-dimensional structures of human, yeast, and oat ubiquitin. J Biol Chem. 1987; 262:6396–6399. [PubMed: 3032965]

Walker JM, Vierstra RD. Ubiquitin-based vectors for the stoichiometric production of multiple proteins in plants. Plant Biotechnol J. 2007; 5:413–421. [PubMed: 17362486]

Wang Y, Griffiths WJ, Jornvall H, Agerberth B, Johansson J. Antibacterial peptides in stimulated human granulocytes: characterization of ubiquitinated histone H1A. Eur J Biochem. 2002; 269:512–518. [PubMed: 11856309]

Washburn MP, Wolters D, Yates JR III. Large-scale analysis of the yeast proteome by multidimensional protein identification technology. Nat Biotechnol. 2001; 19:242–247. [PubMed: 11231557]

Wisniewski JR, Zougman A, Kruger S, Mann M. Mass spectrometric mapping of linker histone H1 variants reveals multiple acetylations, methylations, and phosphorylation as well as differences between cell culture and tissue. Mol Cell Proteomics. 2007; 6:72–87. [PubMed: 17043054]

Wolters DA, Washburn MP, Yates JR III. An automated multidimensional protein identification technology for shotgun proteomics. Anal Chem. 2001; 73:5683–5690. [PubMed: 11774908]

NIH-PA Author Manuscript

NIH-PA Author Manuscript

NIH-PA Author Manuscript

Yan N, Doelling JH, Falbel TG, Durski AM, Vierstra RD. The ubiquitin-specific protease family from Arabidopsis. AtUBP1 and 2 are required for the resistance to the amino acid analog canavanine. Plant Physiol. 2000; 124:1828–1843. [PubMed: 11115897]

Yang P, Fu H, Walker J, Papa CM, Smalle J, Ju YM, Vierstra RD. Purification of the Arabidopsis 26S proteasome: biochemical and molecular analyses revealed the presence of multiple isoforms. J Biol Chem. 2004; 279:6401–6413. [PubMed: 14623884]

Yin XJ, Volk S, Ljung K, et al. Ubiquitin lysine-63 chain forming ligases regulate apical dominance in Arabidopsis. Plant Cell. 2007; 19:1898–1911. [PubMed: 17586653]

NIH-PA Author Manuscript

NIH-PA Author Manuscript

NIH-PA Author Manuscript

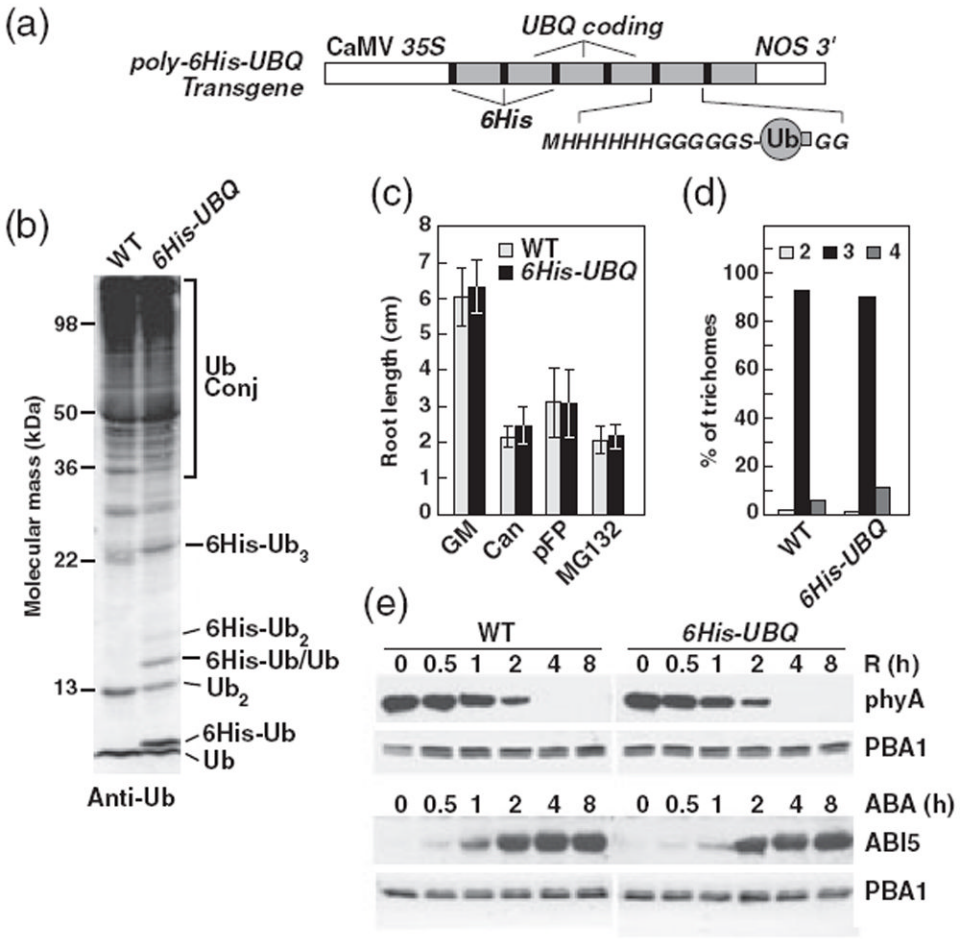

Figure 1. Biochemical and phenotypic analyses of Arabidopsis plants expressing 6xHis-tagged Ub

(a) Diagram of the synthetic *poly-6His-UBQ* gene that directs synthesis of six tandem repeats of 6xHis-tagged Ub expressed under the control of the CaMV *35S* promoter. The sequence of the 6xHis tag added to the N-terminus of each *UBQ* coding region is shown.

(b) Accumulation of 6xHis-tagged Ub in transgenic *6His-UBQ* plants. Equal amounts of crude protein extracts from wild-type and *6His-UBQ* plants were subjected to SDS–PAGE and immunoblot analysis with anti-Ub antibodies. The migration positions of wild-type and 6xHis-tagged Ub monomers, homo- and heterodimers, trimers and higher-molecular-mass Ub conjugates (Ub Conj) are indicated.

(c) Effects of *6His-UBQ* expression on the sensitivity of root growth to 5 μM canavanine (Can), 5 μM *p*-fluorophenylalanine (pFP) or 50 μM MG132. Each bar represents the mean for 18 seedlings (±SE).

(d) Effects of *6His-UBQ* expression on trichome branching. Trichome branch numbers (2, 3 or 4) were recorded for the first true leaves of 14-day-old plants of wild-type and *6His-UBQ* plants. Each bar represents the percentage in each category for at least 10 trichomes measured from each of 20 plants.

(e) Effects of *6His-UBQ* expression on the turnover of two UPS targets – phyA and ABI5. Top: degradation rate of phyA in etiolated seedlings exposed to continuous red light (R) as detected by immunoblot analysis of crude extracts with an anti-phyA monoclonal antibody. Bottom: Accumulation of ABI5 in 5-day-old green seedlings exposed to 50 μM ABA as detected by immunoblot analysis of crude extracts with anti-ABI5 antibodies. Tissue was

collected at the indicated times after red-light or ABA exposure. Immunoblot analyses of the 26S proteasome β1 subunit PBA1 were included to confirm equal protein loading.

NIH-PA Author Manuscript
NIH-PA Author Manuscript
NIH-PA Author Manuscript

NIH-PA Author Manuscript
NIH-PA Author Manuscript
NIH-PA Author Manuscript

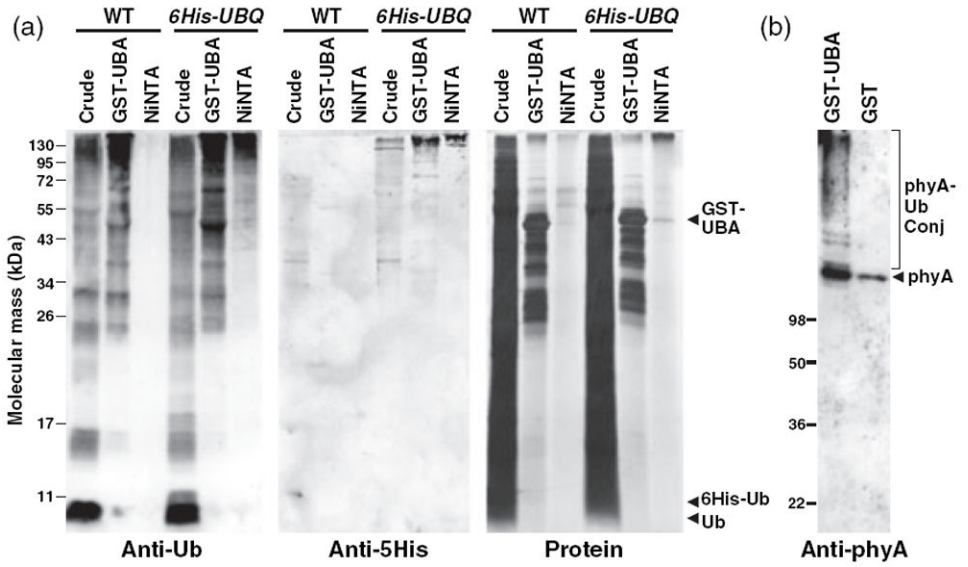

Figure 2. Tandem affinity purification of Ub conjugates from Arabidopsis expressing *6His-UBQ*

(a) Enrichment of Ub conjugates. Crude extracts from 10-day-old green wild-type (WT) and *6His-UBQ* seedlings were subjected to GST–UBA and Ni–NTA chromatography (see Experimental procedures), separated by SDS–PAGE, and either stained for total protein using silver or subjected to immunoblot analysis with anti-Ub or anti-5His antibodies. The arrowheads indicate the migration position of GST–UBA, monomeric Ub and 6xHis-tagged Ub.

(b) Enrichment of phyA–Ub conjugates by GST–UBA affinity chromatography. Five-day-old etiolated wild-type seedlings were irradiated for 1 h with red light, homogenized, and the resulting crude extract was subjected to chromatography on either a GST or GST–UBA column. Bound proteins were eluted with SDS–PAGE sample buffer and subjected to SDS–PAGE and immunoblot analysis with an anti-phyA monoclonal antibody. Non-modified and Ub-conjugated forms of phyA are indicated.

NIH-PA Author Manuscript
NIH-PA Author Manuscript
NIH-PA Author Manuscript

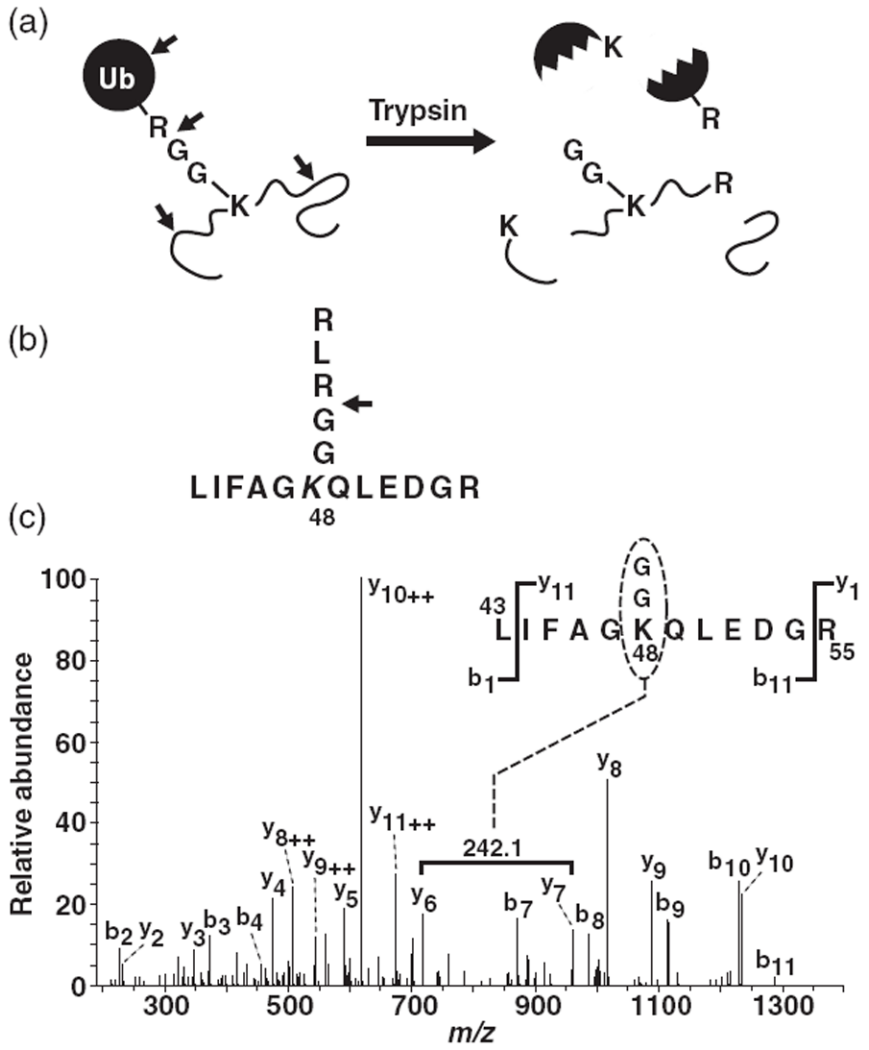

Figure 3. MS/MS identification of Ub conjugation sites

(a) Flow diagram for creating a Ub footprint following digestion of Ub conjugates with trypsin. Arrows show the sites that are predicted to be cleaved by trypsin, generating a peptide containing a lysine (K) that is not cleaved by trypsin and is modified by a di-glycine adduct of 114 Da.

(b) Sequence of a synthetic peptide resembling an internal fragment of Ub containing a second Ub conjugated via an isopeptide bond to Lys48. The arrow indicates the only trypsin cleavage site.

(c) MS/MS spectrum of the Lys48 Ub footprint peptide generated by trypsinization of the peptide shown in (b). The spectrum was generated by collision-induced dissociation of the doubly protonated molecular ion (*m/z* = 730.9) using an ESI ion-trap mass spectrometer. The diagnostic mass shift of 242.1 Da of the modified lysine is indicated.

NIH-PA Author Manuscript

NIH-PA Author Manuscript

NIH-PA Author Manuscript

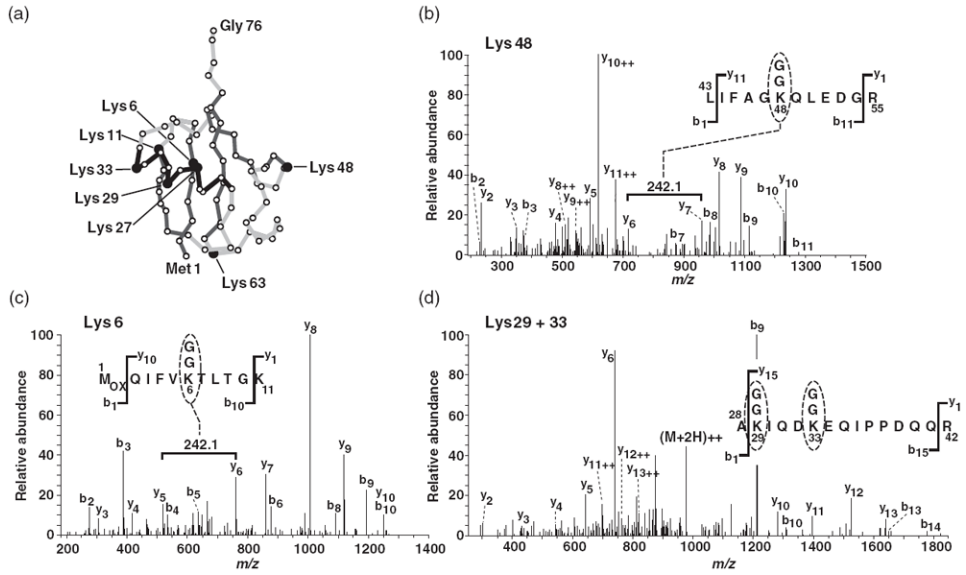

Figure 4. MS/MS identification of Ub attachment sites on Ub itself at Lys48 and Lys6, and evidence for a mixed-linkage Ub chain conjugated at both Lys29 and Lys33

(a) 3D structure of Ub highlighting the positions of the seven lysines (K) in Ub (adapted from Vijay-Kumar *et al.*, 1987). Black, light gray and dark gray lines represent α-helix, β-strand and random coil secondary structures, respectively.

(b–d) MS/MS spectra of the Lys48, Lys6 or Lys29 + 33 Ub footprint peptides obtained from tandem affinity-enriched Ub conjugates after trypsinization. The spectra were generated by collision-induced dissociation of the doubly protonated molecular ions using an ESI ion-trap mass spectrometer. Diagnostic b (N-terminal) and y (C-terminal) ions and the signature mass shift of 242.1 Da for the modified lysines (b,c) are indicated. The subscript ++ indicates doubly charged fragment ions.

(b) Full-size fragmentation spectrum for the molecular ion (*m/z* = 730.9) containing the Ub peptide residues 43-55 with a Ub footprint at Lys48.

(c) Full-size fragmentation spectrum for the molecular ion (*m/z* = 698.4) containing the Ub peptide residues 1–11 with a Ub footprint at Lys6.

(d) Full-size fragmentation spectrum for the molecular ion (*m/z* = 976.0) containing the Ub peptide residues 28–42 with Ub footprints at Lys29 and Lys33. The respective peptide sequence is shown above each spectrum.

NIH-PA Author Manuscript NIH-PA Author Manuscript NIH-PA Author Manuscript

Table 1

Candidate ubiquitylated proteins enriched from Arabidopsis by tandem purification

Locus[a]	Description	# peptides	Homolog[b,c]	Subcell local[d]	X_{corr}	P(Pro)	Mascot
At1g04750	Vesicle-associated membrane protein 721 (AtVAMP7B)	1		Memb	3.95	10^{-5}	
At1g13440	Glyceraldehyde-3-phosphate dehydrogenase (GAPC)	2	*Sc* [2,3]	Cyto	3.28	10^{-6}	
At3g04120			*At* [5]		2.56	10^{-4}	
At1g20693	High mobility group (HMGB2)	1		Nucl	3.48	10^{-5}	
At1g20696	(HMGB3)						
At1g56070	Elongation factor 2, putative (EF-2)	2	*Sc* [2,3]		4.66	10^{-9}	71
					3.07	10^{-2}	56
At1g68100	IAA-alanine resistance protein-1 precursor (IAR1)	1		Memb	5.66	10^{-8}	69
At1g68530	3-ketoacyl-CoA synthase (KCS6)	1		Memb	3.84	10^{-8}	
At1g25450	(KCS5)						
At1g70320	E3 Ub-protein ligase UPL2	1			4.44	10^{-10}	
At1g72450	Jasmonate ZIM domain-containing protein (JAZ6)	1		Nucl	3.60	10^{-6}	41
At1g78570	Rhamnose biosynthesis enzyme (RHM1)	1			3.96	10^{-14}	
At1g53500	(RHM2)						
At3g14790	(RHM3)						
At1g80930	MIF4G & MA3 domains-containing protein	1			3.14	10^{-5}	44
At2g04520	Eukaryotic translation initiation factor 1A	1	*Sc* [2]		3.68	10^{-8}	
At5g35680	(eIF-1A)						
At2g18020	60S ribosomal protein L8 (RPL8A)	2	*Sc* [2]	Cyto	3.20	10^{-5}	
At4g36130	(RPL8C)		*At* [4]		2.49	10^{-2}	
At2g20580	26S proteasome regulatory subunit RPN1a	1	*Sc* [2]	Nucl	2.65	10^{-8}	
At2g36950	Heavy-metal-associated domain- containing protein / putative farnesylated protein	1			3.68	10^{-6}	56
At2g37040	Phenylalanine ammonia-lyase (PAL1)	2		Cyto	2.80	10^{-5}	51
At3g53260	(PAL2)				2.50	10^{-2}	40
At3g10340	(PAL4)						
At2g38230	Pyridoxal biosynthesis protein PDX1.1 (AtPDX1.1)	1		Cyto	5.51	10^{-8}	76
At2g42600	Phosphoenolpyruvate carboxylase (AtPPC2)	1		Cyto	3.59	10^{-7}	

Plant J. Author manuscript; available in PMC 2013 April 29.

NIH-PA Author Manuscript
NIH-PA Author Manuscript
NIH-PA Author Manuscript

Locus[a]	Description	# peptides	Homolog[b,c]	Subcell local[d]	X_{corr}	P(Pro)	Mascot
At1g53310	(AtPPC1)						
At3g05900	Neurofilament protein-related	1			3.50	10^{-7}	51
At3g08530	Clathrin heavy chain	2	*At* [4]	Memb	3.65	10^{-3}	61
At3g11130					2.40	10^{-5}	44
At3g09840	Cell division cycle protein 48 (p97 (CDC48a)	4	*Sc* [1,2]	Nucl + Cyto	3.68	10^{-4}	
At3g53230	(CDC48d)		*At* [4]		3.52	10^{-5}	69
At5g03340	(CDC48e)				2.53	10^{-2}	
					2.50	10^{-5}	34
At3g17390	S-Adenosylmethionine synthetase (SAM3)	2	*Sc* [1,2]	Cyto	2.82	10^{-2}	
At1g02500	(SAM1)		*At* [4]		2.55	10^{-6}	35
At2g36880							
At4g01850	(SAM2)						
At3g19710	Branched-chain-amino-acid aminotransferase 4	2		Cyto	3.56	10^{-6}	81
	(BCAT4)				3.18	10^{-5}	
At3g19820	Cell elongation protein Diminuto-1 (DWF1)	1		Memb	2.97	10^{-5}	47
At3g20770	Ethylene-insensitive 3 (EIN3)	1		Nucl	2.27	10^{-5}	
At3g24503	Aldehyde dehydrogenase 2C4, cytosolic	2		Cyto	2.45	10^{-2}	
	(ALDH1a)				2.24	10^{-4}	55
At3g44310	Nitrilase 1 (NIT1, NRL1)	2	*At* [4]		3.24	10^{-3}	
					2.54	10^{-3}	
At3g50520	Phosphoglycerate/bisphosphoglycerate mutase family	3			3.80	10^{-5}	
At5g04120					3.27	10^{-4}	
					2.77	10^{-5}	
At3g62870	60S ribosomal protein L7a (RPL7aB)	2		Cyto	3.19	10^{-4}	22
At2g47610	(RPL7aA)				2.89	10^{-5}	57
At4g24690	UBA & TS-N & PB1 domains-containing protein	1		Cyto	3.77	10^{-5}	57
At4g25140	Oleosin 18.5 kDa (OLEO1)	2		Memb	2.80	10^{-3}	54
					2.34	10^{-3}	45
At4g27500	Proton pump-interactor 1 (PPI1)	2		ER	3.08	10^{-4}	48
					2.80	10^{-4}	64

Plant J. Author manuscript; available in PMC 2013 April 29.

NIH-PA Author Manuscript
NIH-PA Author Manuscript
NIH-PA Author Manuscript

Locus[a]	Description	# peptides	Homolog[b,c]	Subcell local[d]	X_{corr}	P(Pro)	Mascot
At4g28520	12S cruciferin seed storage protein, putative	3			3.69	10^{-7}	80
	(AtCRU3)				3.37	10^{-8}	58
					3.20	10^{-3}	20
At4g37410	Cytochrome P450, CYP81F4	2	*Sc* [1]	ER	3.64	10^{-3}	
					2.56	10^{-6}	37
At5g01410	Pyridoxal biosynthesis protein PDX1.3 (AtPDX1.3)	1	*At* [5]	Cyto+Memb	4.08	10^{-7}	
At5g02500	Heat shock protein (HSP71)	9	*Sc* [1,2]	Cyto	4.73	10^{-8}	83
At1g16030	(HSP70B)		*At* [4,5]		4.37	10^{-9}	
At1g56410	(HSP70T-1)				3.47	10^{-4}	
At3g09440	(HSP73)				3.10	10^{-4}	60
At3g12580	(HSP70)				2.66	10^{-3}	55
At5g02490	(HSP72)				2.53	10^{-4}	
At5g28540	(BIP1 Luminal-binding protein 1			ER lumen	2.39	10^{-4}	
At5g42020	(BIP2)				2.28	10^{-5}	41
					2.21	10^{-3}	
At5g06600	Ub-specific protease (UBP12)	4			3.35	10^{-6}	
At3g11910	(UBP13)				2.66	10^{-4}	37
					2.42	10^{-3}	
					2.39	10^{-4}	32
At5g40420	Oleosin 21.2 kDa (OLEO2)	1		Memb	3.24	10^{-5}	83
At5g44120	12S seed storage protein, Cruciferina (CRA1)	1			2.83	10^{-8}	69
At5g48930	Transferase family protein	1			4.05	10^{-10}	84
At5g53560	Cytochrome b5 isoform 1 (CYB-51)	1	*Sc* [2]	ER memb	3.57	10^{-10}	
At2g32720	isoform 2 (CYB-52)						
At5g56010	Heat shock protein 81 (HSP81-3)	2	*Sc* [2]	Cyto	3.27	10^{-5}	
At5g56000	(HSP81-4)		*At* [4]		2.20	10^{-3}	
At5g56030	(HSP81-2)						
At5g52640	(HSP81-1)						
At5g60390	Elongation factor 1-alpha	1	*Sc* [2]	Cyto	2.71	10^{-7}	49
At1g07930	(EF1A)		*At* [4,5]				

Plant J. Author manuscript; available in PMC 2013 April 29.

NIH-PA Author Manuscript NIH-PA Author Manuscript NIH-PA Author Manuscript

Locus[a]	Description	# peptides	Homolog[b,c]	Subcell local[d]	X_{corr}	P(Pro)	Mascot
At1g07940							
At1g07920							
At5g60790	General control non-repressible 1 (GCN1) ABC transporter	1			3.05	10^{-5}	83
At5g62390	BCL-2-associated athanogene 7 (BAG7)	2			2.70	10^{-7}	
					2.59	10^{-3}	

[a] Genes including the identified peptide sequence, underlined represents most expressed gene based on EST numbers.

[b] Ub-conjugate identified in homologous protein from *Saccharomyces cerevisiae* (*Sc*). References: [1] (Peng *et al.*, 2003) and [2] (Mayor *et al.*, 2005) and [3] (Tagwerker *et al.*, 2007).

[c] Reported as putative Ub-conjugate in *Arabidopsis thaliana (At)*. References: [4] (Maor *et al.*, 2007) and [5] (Manzano *et al.*, 2008).

[d] Subcellular localization of protein from annotation of protein/gene in SwissProt or NCBI nr.

Cyto, cytoplasm; ER, endoplasmic reticulum; Nucl, nucleus; Memb, membrane.

Plant J. Author manuscript; available in PMC 2013 April 29.

NIH-PA Author Manuscript NIH-PA Author Manuscript NIH-PA Author Manuscript

Table 2

a. Ubiquitylated Arabidopsis proteins with canonical Ub footprint s[a]

Locus[c]	Description	Peptide seq[d]	Ub-site[e]	Homol[f,g]	Subcell loc[h]	X_{corr}	P(Pro)	Mascot
At1g04410	Malate dehydrogenase (MDHC1)	SQAAALEK(ub) HAAPNC*K	Lys119 of 1519	*Sc* [1]	Cyto	3.77	10^{-8}	79
				Hs [6]				
At1g09310	Expressed protein	AK(ub) AEMYTGDEIC*R	Lys15 of 179			3.40	10^{-6}	64
At2g01720	Ribophorin I family	K(ub) SELEFEPR	Lys310 of 464			2.59	10^{-3}	48
At2g30620	Histone H1.2	GK(ub) VAAAVAPAK	Lys156	*Hs*+mouse [3]	Nucl	3.03	10^{-3}	53
		VAAAVAPAK(ub) AK	Lys165 of 273	*Hs* [4,5]		2.97	10^{-4}	42
At3g53870	40S ribosomal protein S3 (RPS3B)	TQNVLGEK(ub) GR	Lys62 of 250	*Sc* [2]	Cyto	2.57	10^{-2}	43
At2g31610	(RPS3A)	+ 1 other peptide		*Hs* [6]		3.25	10^{-3}	31
At5g35530	(RPS3C)							
At4g24110	Unknown protein	VVK(ub) GGDVIYGSR	Lys73 of 250			2.74	10^{-6}	
At4g37410	Cytochrome P450, CYP81F4	AAAK(ub) VIDEM*LQR + 2 other peptides (Table I)	Lys245 of 501	*Sc* [2]	ER	3.00	10^{-3}	37
At5g02500	Heat shock protein (HSP71)	TK(ub) DNNLLGK	Lys457 of ~650	*Sc* [1,2]	Cyto	2.30	10^{-4}	37
At3g09440	(HSP73)	+9 other peptides (Table I)		*At* [7,8]				
At3g12580	(HSP70)			*Hs* [6]				
At5g02490	(HSP72)							
At5g17920	Methionine synthase (MS1,METE)	AAAALK(ub) GSDHR	Lys406 of 765	*At* [8]	Cyto	3.19	10^{-7}	63
At3g03780	(MS2)	+ 1 other peptide				2.85	10^{-3}	36
At5g60390	Elongation factor 1-alpha (EF1A)	DPTGAK(ub) VTK(ub) AAVK	Lys438 + Lys441 of 449	*Sc* [1]	Cyto	2.29	10^{-2}	26
At1g07930				*At* [7,8]				
At1g07940		+ 1 other peptide (Table I)						
At1g07920								
b. Ubiquitylated Arabidopsis proteins with non-canonical Ub footprint(s)[b]								
At1g13110	Cytochrome P450 71B7	FGPVM*LLHFGFVPVVVISSK(ub)	Lys82 of 504	*Sc* [2]	Memb	2.23	10^{-4}	
At1g72150	Patellin-1 (PATL1, SEC14)	EALTMLKNTVQWRK(ub)	Lys285 of 573		Memb + Cyto	2.22	10^{-3}	
		+ 1 other peptide				2.61	10^{-3}	46
At4g14140	DNA methyltransferase 2 (MET2)	M*QDIHHTKWIIKK(ub)	Lys583 of 1519			2.29	10^{-4}	

Plant J. Author manuscript; available in PMC 2013 April 29.

NIH-PA Author Manuscript
NIH-PA Author Manuscript
NIH-PA Author Manuscript

Locus[c]	Description	Peptide seq[d]	Ub-site[e]	Homol[f,g]	Subcell loc[h]	X_{corr}	P(Pro)	Mascot
c. Ubiquitin with canonical Ub footprint(s)[a]								
Ubiquitin		MQIFVK(ub) TLTGK	Lys6			2.35	10^{-3}	
		M*QIFVK(ub) TLTGK	Lys6			3.84	10^{-5}	
		TLTGK(ub) TITLEVESSDTIDNVK	Lys11			4.58	10^{-11}	
		AK(ub) IQDKEGIPPDQQR	Lys29			5.18	10^{-9}	
		IQDK(ub) EGIPPDQQR	Lys33			2.55	10^{-7}	48
		AK(ub) IQDK(ub) EGIPPDQQR	Lys29+Lys33			2.92	10^{-3}	
		LIFAGK(ub) QLEDGR	Lys48			4.32	10^{-8}	85
		LIFAGK(ub) QLEDGRTLADYNIQK	Lys48			4.99	10^{-10}	
		TLADYNIQK(ub) ESTLHLVLR	Lys63			2.84	10^{-6}	

[a] Canonical Ub footprint was defined as a lysine with an additional m/z of 114 that was not cleavage by trypsin.

[b] Non-canonical Ub footprint was defined as a lysine with an additional m/z of 114 that was at the end of the peptide following trypsin digestion.

[c] Genes including the identified peptide sequence, underlined represent most expressed gene (EST).

[d] K(ub), ubiquitylated Lys (Lys with footprint) ; C*, carbamidomethylated Cys; M*, oxidized Met.

[e] Ub-site of protein length (aa).

[f] Ub-conjugate identified in homologous protein from *Homo sapiens* (*Hs*) *or Saccharomyces cerevisiae* (*Sc*). References: [1] (Mayor *et al.*, 2005) [2] (Peng *et al.*, 2003), [3] (Wisniewski *et al.*, 2007), [4] (Wang *et al.*, 2002), [5] (Denis *et al.*, 2007) and [6] (Matsumoto *et al.*, 2005).

[g] Reported as putative Ub-conjugate in *Arabidopsis thaliana (At)*. References: [7] (Maor *et al.*, 2007) and [8] (Manzano *et al.*, 2008).

[h] Subcellular localization of protein from annotation of protein/gene in SwissProt or NCBI nr; Cyto, cytoplasm; ER, endoplasmic reticulum; Nucl, nucleus; Memb, membrane.

Plant J. Author manuscript; available in PMC 2013 April 29.

NIH-PA Author Manuscript

NIH-PA Author Manuscript

NIH-PA Author Manuscript

Table 3

Detection of Ub–Ub linkages in Arabidopsis[a]

			Values in Maor *et al.* (2007)	
Intra-Ub–Ub linkage	**Number of peptides**	**Percentage of total**	**Number of peptides**	**Percentage of total**
Lys6	4	1.0	0	0.0
Lys11	15	3.8	28	8.9
Lys27	0	0.0	0	0.0
Lys29	19	4.8	8	2.6
Lys33	3	0.8	19	6.1
Lys29 + Lys33	1	0.3	0	0.0
Lys48	354	89.2	197	62.9
Lys63	1	0.3	61	19.5
Total	397		313	

[a]Data from the present study were assembled from five independent MS/MS analyses.